Available online at www.sciencedirect.com
SCIENCE DIRECT
Physica D 218 (2006) 158–166
PHYSICA D
www.elsevier.com/locate/physd

Rayleigh–Taylor instability of pulled versus pushed fronts

D. Lima[a], W. van Saarloos[b], A. De Wit[a,*]

[a] *Service de Chimie Physique et Biologie Théorique and Centre for Nonlinear Phenomena and Complex Systems, CP231, Université Libre de Bruxelles, Campus Plaine, 1050 Brussels, Belgium*
[b] *Instituut-Lorentz, Leiden University, Postbus 9506, 2300 RA Leiden, The Netherlands*

Received 7 February 2006; received in revised form 3 May 2006; accepted 3 May 2006
Available online 13 June 2006
Communicated by C.K.R.T. Jones

Abstract

Due to a possible density difference across an autocatalytic reaction–diffusion front, a hydrodynamic Rayleigh–Taylor instability triggering fingering of the self-organized interface can set in when the front is propagating perpendicularly to the gravity field. We investigate here the influence of the form of the reaction kinetics on the stability properties and the nonlinear dynamics of fingering. We show that the pulled versus pushed character of the front leads to important differences in the dispersion curves and in the role of fluctuations in the nonlinear dynamics of fingering. In particular, the effective dispersion curve in the pulled regime is strongly time-dependent, and only converges to the usual dispersion relation of the Rayleigh–Taylor instability at late times. Our results also have implications for combustion fronts.

Keywords: Rayleigh–Taylor instability; Pulled fronts; Pushed fronts

1. Introduction

When a chemical reaction front is propagating in a solution, the density before and behind the front will generally be different. As a result, even when the chemical front itself has no diffusive instabilities, a long-wavelength Rayleigh–Taylor-like (RT) instability can occur in a vertical cell, if the front is such that it results in a heavier solution being on top of a lighter one. Many authors have studied this situation in the last few years, both experimentally and theoretically ([1–3] and references therein). The details generally depend on the size and aspect ratio of the cell and on the precise form of the reaction equation. However, in the limit that the cell is much larger than the intrinsic front width, the problem simplifies and depends only on a few effective parameters, as in this limit the front dynamics can normally be mapped onto that of an infinitely sharp interface — the problem then essentially reduces to the usual Rayleigh–Taylor instability of a sharp reactive interface. The techniques to map a moving front onto a sharp interface description go under various names (moving boundary approximation, sharp or effective interface limit, eikonal approximation), but are well known and applied in many fields. In essence, the technique comes down to a matched asymptotic expansion in which the dynamics on the "inner" front scale is translated into effective boundary conditions for the dynamics of the effective interface on the "outer" scale [4–8].

The effective interface approach leads one intuitively to expect the details of the chemical reaction to have only minor consequences. A comparison between experimental dispersion curves (giving the growth rate of the RT instability as a function of its wave number) for fingering of iodate–arsenous acid (IAA) [9] and chlorite–tetrathionate (CT) [10] reactions show that they feature strong similarities. Theoretical dispersion curves computed for third-order [11–13] and fourth-order [14,15] one-variable models describing respectively the IAA and CT reactions in the experimental conditions also present similar characteristics. These curves predict therefore the onset of fingers with analogous wavelength at roughly the same time in both systems. Experimental analysis of the nonlinear fingering dynamics of IAA [2] and CT [3] fronts show similar regimes of coarsening, merging and sometimes finger splitting. Numerical integration of the corresponding third-order [1] and

* Corresponding author.
E-mail addresses: saarloos@lorentz.leidenuniv.nl (W. van Saarloos), adewit@ulb.ac.be (A. De Wit).

0167-2789/$ - see front matter
doi:10.1016/j.physd.2006.05.002

fourth-order [14,16] models also point out similar nonlinear dynamics such as evolutions towards one asymptotic single finger with self-similar properties (which could be mapped onto a sharp interface description) and onset of tip-splitting above a given critical value of parameters. However, one surprising and hitherto unexplained finding has been that if indeed the cell is wide, so that an interfacial description would be expected to apply, there are nevertheless important differences between the stability and dynamics of fingering of fronts with "quadratic" autocatalysis reaction kinetics (e.g. Eq. (6) below) and "cubic" or higher-order autocatalysis (e.g. Eq. (7) below) [17–19]. For example, in a careful study of Coroian and Vasquez [18], it was found that going from cubic to higher-order autocatalytic reactions only induces very small shifts in the critical Rayleigh number at which the front becomes unstable in wide cells, while in their widest cells the critical Rayleigh number was found to be about three times as big when they switched from cubic to quadratic kinetics. In other words, fronts with order two kinetics were found to be much more stable with regard to fingering than higher-order ones which converged to the results for an eikonal relation in wide cells.

It is the goal of this paper to put these findings into a more general perspective by explaining the origin of the differences of fingering properties between order two and larger order kinetics in terms of the differences between so-called *pulled* and *pushed* fronts [20]. Indeed, it has become clear in recent years that fronts which propagate into a linearly unstable state come simply in two classes: pulled fronts whose dynamics is driven by the linear instability *ahead of the actual front itself* and pushed fronts whose dynamics are driven by the nonlinearities in the front region itself. Strictly speaking, only the latter type of fronts reduce to a moving boundary approximation in the thin interface limit — pulled fronts do not. Due to the fact that the dynamics of pulled fronts are governed by what happens in the semi-infinite region *ahead* of them, their velocity converges very slowly to their asymptotic value [21], and the same feature implies that we can formally not map them mathematically onto a moving boundary problem [8]. The implications of this in a given practical case are not immediately clear. Some pulled fronts become indeed very sensitive to noise or slight changes in the equations [20], but in other cases it appears that an empirical moving boundary (or thin front) approximation still leads to sensible results for the stability of the fronts, provided one takes into account that the convergence of the pulled fronts to their asymptotic speed and shape is quite slow. The results of Coroian and Vazquez [18] and similar results for combustion fronts [22] indicate that this is the case with chemical and combustion fronts. Indeed, as we shall see in this paper, for the "quadratic" autocatalytic fronts with a Rayleigh–Taylor instability, the main implication of the pulled nature of these fronts appears to be that the Rayleigh–Taylor instability emerges only very slowly in time, much slower than in the pushed regime. In addition, there is an enhanced sensitivity to initial conditions. As a result, even though the instability threshold is difficult to define sharply for pulled fronts, as initial conditions remain more important, we can understand the increased stability of fronts with quadratic kinetics in terms of the slow convergence of their speed to the asymptotic value: for a long time the dispersion relation of a pulled front is dominated by the slow acceleration of the front velocity to its asymptotic value, and during this phase the buoyancy-induced long-wavelength instability is suppressed.

This article is organized as follows. In Section 2, we present the model to be used to analyze RT fingering of chemical fronts and introduce two different kinetics yielding respectively a pushed and a pulled front. In Section 3, we contrast the nonlinear fingering dynamics of pushed versus pulled fronts. To enlighten the differences observed, we recall in Section 4 the known main differences between both families of fronts. On the basis of this explanation, we revisit fingering of pushed versus pulled fronts in Section 5, where we compare the dispersion curves of both systems before concluding in Section 6.

2. Model and numerical technique

As we mentioned above, reaction–diffusion pushed fronts converge to their asymptotic speed exponentially fast on the time scale of the intrinsic front relaxation time, while pulled fronts do not. In this section we investigate the nonlinear behaviour of both types of fronts with regard to buoyancy-driven fingering.

The problem can be described using a two-dimensional model system of width L_y and length L_x oriented vertically along the gravity direction $\underline{e}_x$, with y the transverse direction. A chemical front is initiated at the bottom and propagates upwards in the $-x$ direction. We will make the problem dimensionless using scales based on the velocity $U = \Delta\rho g K/\nu$, the length $L_h = D_m/U$ and the time $\tau_h = D_m/U^2$. Here $\Delta\rho$ is the dimensionless density difference across the front, g the gravity acceleration, K the permeability, while D_m is the diffusion coefficient of the relevant chemical species and $\nu = \mu/\rho_o$ is the kinematic viscosity of the solvent with μ and ρ_o being its dynamic viscosity and density respectively. The pressure p, density ρ and concentration c are scaled using $\mu D_m/K$, $(\rho_2 - \rho_1)$ and c_o, where ρ_2 and ρ_1 are the densities of the heavy and light solutions respectively and c_o is the initial concentration of c. The hydrostatic pressure gradient is incorporated in $\underline{\nabla} p$. The dimensionless Damköhler number, Da, is introduced as the ratio of the hydrodynamic time scale τ_h to the chemical time scale $\tau_c = 1/(q c_o^n)$, where q is the kinetic constant and n the order of the kinetics. The dimensionless equations written using these scales take the form [1,11,14,16]:

$$\underline{\nabla} \cdot \underline{u} = 0, \tag{1}$$

$$\underline{\nabla} p = -\underline{u} + (1 - c)\underline{e}_x, \tag{2}$$

$$\frac{\partial c}{\partial t} + \underline{u} \cdot \underline{\nabla} c = \nabla^2 c + Da f(c). \tag{3}$$

The second equation is Darcy's law for the incompressible velocity field $\underline{u}$. The density of the solution is assumed to depend linearly on the concentration c which varies according to the reaction–diffusion–advection equation (3). This system of equations describes the evolution of a chemical front propagating into a 2D porous medium or a thin Hele–Shaw cell. In dimensionless units, the length is now $L'_x = L_x/L_h$ while

the dimensionless width of the system is basically the Rayleigh number of the problem defined as

$$Ra = \frac{L_y}{L_h} = \frac{\Delta\rho g K L_y}{\nu D_m}. \tag{4}$$

We have studied this system for two different kinetics $f(c)$ which are special cases of the cubic polynomial

$$f(c) = a_1 c + a_2 c^2 + a_3 c^3, \quad (a_1 > 0), \tag{5}$$

with the coefficient of the highest-order nonzero term negative. The condition that $a_1 > 0$ implies that the stationary state $c = 0$ is *unstable*, and the condition that the highest-order nonzero coefficient is negative implies that there always is a stationary state with $c > 0$. The examples discussed in this paper are

$$a_1 = 1, \quad a_2 = -1, \quad a_3 = 0: \quad f(c) = -c(c-1), \tag{6}$$

$$a_1 = 0.01, \quad a_2 = 0.99, \quad a_3 = -1: \quad f(c) = -c(c-1)(c+0.01) \tag{7}$$

which are examples of "quadratic" and "cubic" autocatalysis, respectively. The kinetics (7) corresponds to the one used to model the iodate–arsenous acid (IAA) reaction. As will be discussed more explicitly in Section 4 below, this reaction kinetics leads to so-called pushed fronts, which in the absence of convection, move with velocity $v_{rd} = 0.721$. The second-order kinetics (6) could be due to a chemical reaction of the type A + B → 2B [17], and leads to so-called pulled fronts. The corresponding asymptotic reaction–diffusion front speed is $v_{rd} = 2$. Studies of other pulled and pushed kinetics fully confirm the tendencies to be explained below on the basis of the examples (6) and (7) and are therefore not reported here.

In order to numerically integrate the set of Eqs. (1)–(3) with $f(c)$ given by Eqs. (6) and (7), we introduce the stream function ψ such that $u = \partial\psi/\partial y$ and $w = -\partial\psi/\partial x$. In terms of this variable, the equations of the problem become:

$$\nabla^2\psi = -c_y, \tag{8}$$

$$c_t + c_x\psi_y - c_y\psi_x = \nabla^2 c + Daf(c), \tag{9}$$

where subscripts indicate partial derivatives. Eqs. (8) and (9) are solved using a pseudo-spectral method [1,14,16,23] on a two-dimensional domain, the dimensionless length and width of which are given by L'_x and Ra respectively. Note that the Rayleigh number only appears implicitly in the problem through the lateral width of the cell, see Eq. (4). We impose periodic boundary conditions in both directions. The initial condition is a step function along x going from $c = 1$ to $c = 0$ and located at the bottom of the system with a noise applied at the front, at an intermediate concentration between $c = 0$ and $c = 1$. To ensure periodicity in agreement with our periodic boundary condition, a reverse step function going from $c = 0$ to $c = 1$ is constructed at the top as well. For some of the simulations, we have created a drop of nonzero c ahead of the upward moving front. To visualize the dynamics, we plot the two-dimensional concentration field on a grey scale ranging from black ($c = 0$) to white ($c = 1$). The systems are always taken long enough so that the dynamics observed does not depend on the front meeting any boundary or the other front. However, for clarity, we show only a focus on the unstable concentration field of the upward propagating front in order to better visualize the results under discussion.

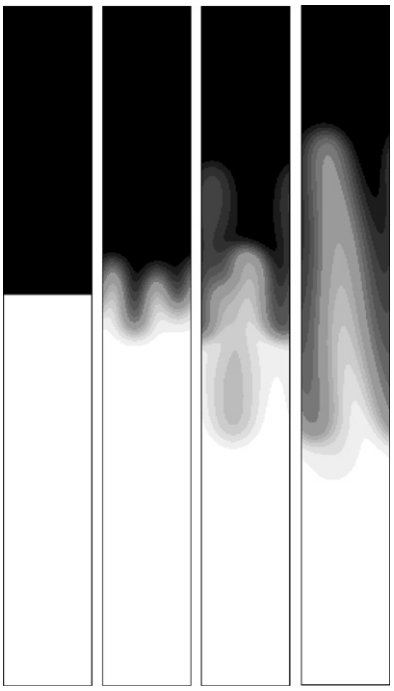

Fig. 1. Pure Rayleigh–Taylor density fingering for $f(c) = 0$, $Ra = 256$ shown at times $t = 0$, 3000, 6000 and 9000.

3. Nonlinear dynamics of fingering

Fig. 1 shows pure density fingering in the absence of chemical reactions, i.e. for $f(c) = 0$. The fingers develop without a preferential direction (neither up nor down) from the initial position of the front corresponding to the heavy $c = 0$ fluid overlying the light $c = 1$ solution. Let us compare this with fingering of chemical fronts. The case where $f(c)$ is given by Eq. (7) is shown in Fig. 2. We focus on the unstable ascending front and one can see the interplay between the reaction–diffusion processes and the hydrodynamics. The fingers now favor the upgoing direction of the advancing front. Their initial wavelength is in good agreement with the one predicted by the linear stability analysis. Through a coarsening dynamics [24] these initial fingers merge, leading to one asymptotic finger, the shape and speed of which do not undergo further changes [1,16]. This front is pushed and in the presence of convection it advances with a front speed $v > v_{rd}$. In Fig. 3 we can see the evolution of a pulled front, corresponding to the kinetics $f(c) = -c(c-1)$. The initial condition, as for all our simulations here, is a step function and after a relaxation of the initial steep front only one single finger emerges.

We have investigated the effect of a small perturbation ahead of the front. In order to do so, we have set a nonzero c in a small localized region well ahead of the step condition. We have tested our results for c varying in the perturbation in the range $10^{-3} \leq c \leq 0.2$. For the case of pure density

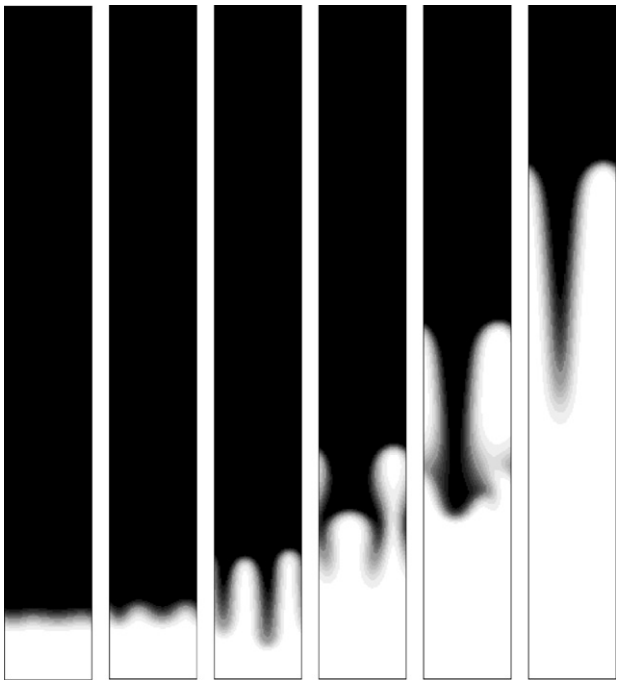

Fig. 2. Density fingering for the pushed kinetics $f(c) = -c(c-1)(c+0.01)$, $Ra = 256$, $Da = 0.01$. The nonlinear evolution of the concentration c is shown at successive times $t = 1089$, 1287, 1881, 2772, 3762 and 5049.

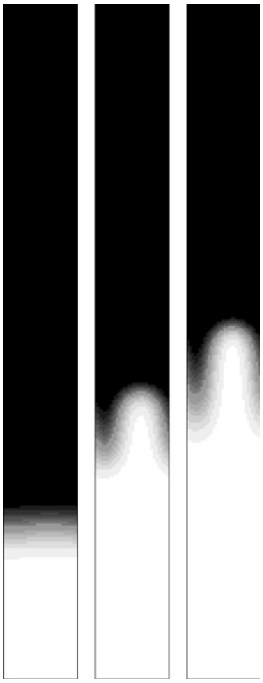

Fig. 3. Density fingering for the pulled kinetics $f(c) = -c(c-1)$, $Ra = 256$, $Da = 0.0005$ shown at times $t = 1485$, 2475 and 2871.

fingering there was no growing of the perturbation. For the pushed front kinetics $f(c) = -c(c-1)(c+0.01)$, these small perturbations grow very slowly and are systematically *overtaken* by the ascending front, even for large c at the drop position.

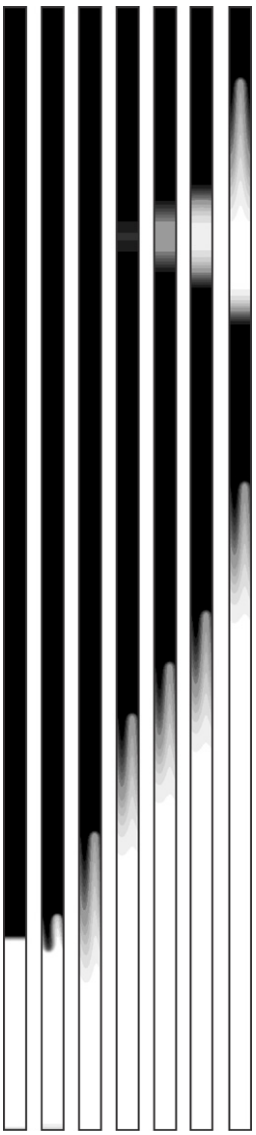

Fig. 4. Density fingering for $f(c) = -c(c-1)$, $Ra = 256$, $Da = 0.0005$ in the presence of a drop of $c = 0.1$ placed at $t = 0$ ahead of the front. The density plots show the variable c for successive times $t = 400$, 4000, 9000, 18 000, 22 000, 26 000 and $t = 36\,000$.

When we placed the small drop in a system presenting pulled fronts, we have observed that the perturbation grows quickly and gives rise to another front. Such dynamics can be seen in Fig. 4. At the lower part of the plots, we can see the same fingering dynamics as for the system without the *drop*. At the upper part, the initially localized perturbation grows, giving rise to both a stable downward propagating front and an unstable front moving upwards and evolving also into an asymptotic single finger traveling at the same faster speed than the first finger.

The difference between the two cases illustrates that while the front velocities are not that different ($v^\dagger \approx 0.721$ according to Eq. (15) below in the first case and $v^* = 2$ in the pulled regime of Fig. 4), the exponential growth rate for small perturbations about the unstable state is a factor 100 different

in the two regimes[1] (growth $\sim e^{0.01t}$ in the first case, e^t in the second one).

4. One-dimensional dynamics of pulled and pushed fronts

In order to understand the effect of the reaction kinetics on the long-wavelength RT stability and dynamics of the reaction fronts studied in the previous section, it is important to summarize the most important findings of the study of the general problem of front propagation into unstable states, as reviewed in [20].

For our situation, the relevant question concerning front selection is the following: what is the long-time velocity of fronts that propagate into an unstable domain where $c = 0$, if they emerged from initial conditions which are such that, at $t = 0$, c decayed to zero fast enough when going into the unstable domain. For the precise formulation of such so-called "sufficiently localized" initial conditions, we refer to [20]; for here it is sufficient to know that decay to zero at least as fast as a Gaussian is always fast enough.[2]

An important aspect of fronts which propagate into a linearly unstable state is the following. When a state is linearly unstable, this means that when the equations are linearized about this stationary state, a range of Fourier modes of the form $e^{-i\omega t+ikx}$ will be unstable, i.e. will have $\mathrm{Im}\,\omega(k) > 0$. Because of the instability, even a small perturbation about the unstable state will grow out and spread, according to the linear dynamics. This linear spreading can be solved exactly for any equation — in general the asymptotic *linear spreading speed* v^* is given by the equations

$$\left.\frac{\mathrm{d}\omega}{\mathrm{d}k}\right|_{k^*} = \frac{\mathrm{Im}\;\omega(k^*)}{\mathrm{Im}\;k^*} = v^*. \tag{10}$$

Notice that the first equality effectively constitutes two equations, for the real and imaginary part of k^*, and the second equality then determines the linear spreading velocity v^*.

The linear spreading problem is so robust that it determines to a large extent the dynamics of fronts that propagate into an unstable state. Indeed, the general answer from the theory of front propagation is simply the following: quite generally, for front propagation into unstable states, only two regimes are possible. Either the dynamically selected fronts are "*pulled fronts*" whose asymptotic speed is equal to the linear spreading speed v^*, or they are "*pushed fronts*" whose asymptotic speed is higher than the linear spreading speed v^*. Only in the pushed regime is the velocity dependent on all of the nonlinearities in the equation — as long as fronts are pulled their speed is completely independent of the nonlinearities in the equation. Even though a general analytic result is not known, generally speaking for a front to be pushed (and hence faster than v^*), the nonlinearities need to enhance the growth over that given by the linear terms.

There are many important differences between the pulled and pushed regime. Pushed fronts converge to their asymptotic speed exponentially fast (as their linear stability spectrum is gapped), and as a result when one considers a pushed front in more than one dimension, whose radius of curvature is much less than the front thickness, the motion of such a front can be mapped onto a moving boundary problem (sometimes also called an effective interface description but often called an eikonal description in the literature on chemical fronts). The dynamics of pulled fronts, on the other hand, is dominated not by what happens in the nonlinear front region, but actually by what happens in the region *ahead of the front!* Because of this, even if a weakly curved pulled front in more than one dimension looks thin on the scale of its radius of curvature, *its dynamics can not be mapped onto a moving boundary (eikonal) formulation* [8,20,27]. This formulation is also called the "thin front limit" in the flame literature [22].

Another aspect of the fact that the dynamics of pulled fronts is actually driven by what happens ahead of the actual nonlinear front region is that their velocity relaxes only very slowly to their asymptotic value v^*: for fronts like those considered here which converge to uniformly translating fronts the asymptotic behavior for the time-dependent velocity $v(t)$ is given by [20, 21]

$$v(t) = v^* - \frac{3}{2\lambda^* t} + \frac{3\sqrt{\pi}}{2\sqrt{D}(\lambda^*)^2 t^{3/2}} + \mathcal{O}\left(\frac{1}{t^2}\right), \tag{11}$$

where

$$\lambda^* = \mathrm{Im}\;k^*, \quad D = \frac{\mathrm{i}}{2}\left.\frac{\mathrm{d}^2\omega(k)}{\mathrm{d}k^2}\right|_{k^*}. \tag{12}$$

Both of these crucial features of pulled fronts, the fact that even if they are thin they do not converge to a moving boundary problem and the fact that their speed converges very slowly to the asymptotic value v^*, also emerge in the fingering of chemical reaction fronts studied above. Before discussing this, we specialize these general findings to the reaction fronts studied here.

For our fronts, the relevant application of these findings concern fronts in the one-dimensional reaction diffusion equation

$$\frac{\partial c}{\partial t} = \frac{\partial^2 c}{\partial x^2} + f(c), \tag{13}$$

with $f(c)$ given by Eqs. (6) and (7). Here a_3 needs to be negative to ensure saturation behind the front, and we take $a_2 > 0$ for convenience.

Even though for most equations and even for the reaction diffusion Eq. (13) with general function $f(c)$ the transition

[1] The difference is even more significant if the term linear in c in $f(c)$ is absent, e.g. if $f(c) = -c^2(c-1)$. In this case, the growth for small c is only algebraic and two dimensions is the boundary between having a threshold on the perturbation for growth — in other words, in three dimensions only perturbations above a certain threshold grow out. Effectively, there is a "nucleation barrier" in three dimensions [25].

[2] To be more precise, we consider perturbations which in the pulled regime fall off faster than $\exp(-\lambda^* x)$ for $x \to \infty$ with λ^* given in (12) below [20]. Initial conditions which fall off slower lead to larger front speeds. For example, if the initial condition falls of as $\exp(-ax)$, then the asymptotic front speed is $v_{as} = a + a_1 a^{-1}$. See in particular Ref. [26] for a discussion of such generalizations in the context of reaction diffusion equations.

from pulled to pushed is not known analytically, for the case (5) the pushed velocity and front shape is known analytically [21]: for fronts with $c \geq 0$ the fronts are pushed when

$$a_2 > \sqrt{|a_3|a_1/2}, \quad (a_3 < 0), \tag{14}$$

and the speed $v^\dagger$ and steepness $\lambda^\dagger$ of the pushed front are then given by

$$v^\dagger = \frac{1}{4}\left(\frac{a_2}{|a_3|}\right)^{3/2}\left(-1+3\sqrt{1+4R}\right)\left(1+\sqrt{1+4R}\right)^{1/2}, \tag{15}$$

$$\lambda^\dagger = \frac{a_2^{3/2}}{4|a_3|}\left(1+\sqrt{1+4R}\right)^{3/2}, \tag{16}$$

where

$$R = \frac{a_1|a_3|}{a_2^2} < 2, \tag{17}$$

and where in the comoving frame $\xi = x - v^\dagger t$, the asymptotic front profile is

$$c(\xi) = \frac{a_2^{1/2}}{2|a_3|}\left(1+\sqrt{1+4R}\right)\frac{1}{1+e^{\lambda^\dagger(\xi-\xi_0)}} \tag{18}$$

with ξ_0 arbitrary due to translation invariance. In the pulled regime, i.e. when (14) is not obeyed, the velocity and steepness are simply

$$v^* = 2\sqrt{a_1}, \quad \lambda^* \equiv \mathrm{Im}\, k^* = \sqrt{a_1}, \tag{19}$$

but the asymptotic front profile is not known in closed analytic form.

According to these results, the first case (6) (with $a_2 < 0$) correspond to pulled front, and the second one (7) (with $R \approx 0.01$) is in the pushed regime. We illustrate the above summary of the difference in the front dynamics in these two regimes with numerical simulations. In Fig. 5, the pulled and pushed fronts are shown at different times, and one can see how the steep step-function initial condition relaxes to the smoother asymptotic front solution. In Fig. 6 we have plotted the instantaneous front speeds of both pushed and pulled fronts as a function of time. These are calculated in time as the tangent to the curve of the location of one given concentration of the profile as a function of time. The horizontal lines show the asymptotic front speeds, as calculated analytically. The difference in the front speed evolution for pulled and pushed fronts is indeed striking: pushed fronts reach their asymptotic speed quite quickly, while pulled fronts experience a very slow relaxation as compared to their pushed counterparts. On comparing the time-dependence of the pulled fronts with the analytic predictions, one should keep in mind that the exact asymptotic result (11) normally becomes accurate only at much later times than those shown in the figure.

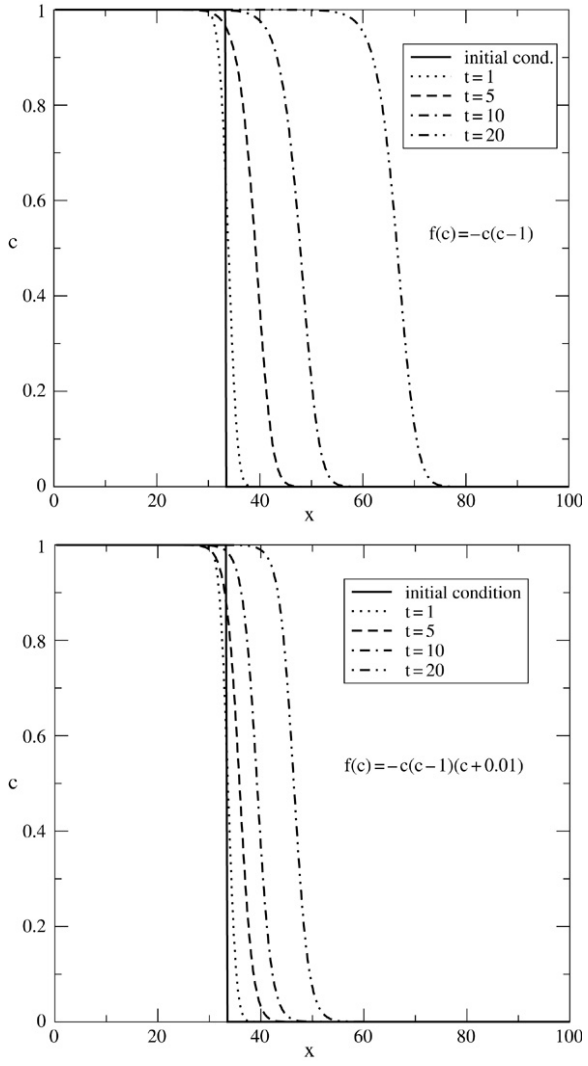

Fig. 5. Front profiles for both pulled (top) and pushed (bottom) kinetics shown at the same successive times starting from a step function as an initial condition.

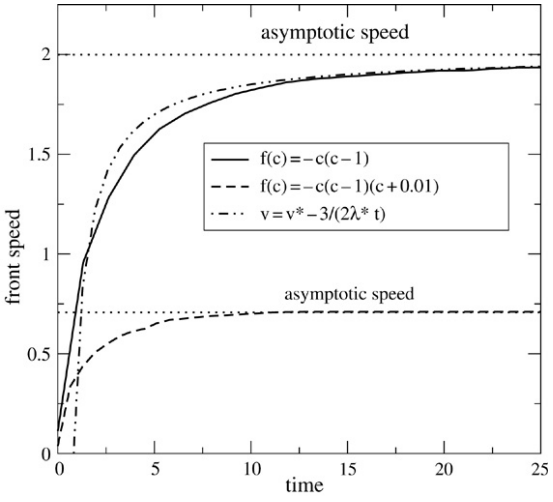

Fig. 6. Front speeds as a function of time for the pushed and pulled fronts. The analytical solution up to the leading term of Eq. (10) is also plotted. The speed of the pushed front converges much more rapidly to its asymptotic value than that of the pulled one.

5. Linear stability analysis of pulled and pushed fronts

In order to explore the implications of the difference in behavior of pushed versus pulled fronts when their dynamics

depends on buoyancy effects, we now perform a linear stability analysis of these different fronts with regard to the buoyancy-driven Rayleigh–Taylor instability in a moving coordinate $z = x - vt$. In order to do a linear perturbation theory for lateral modulations of the front, we first generate unperturbed flat fronts corresponding to the one-dimensional base state:

$$c_0 = c_0(z, t), \tag{20}$$

$$\underline{u} = 0, \tag{21}$$

$$p_0 = p_0(z, t), \tag{22}$$

where p_0 is the pressure profile for a given c_0. Then we perturb the base state and expand in Fourier modes the perturbations velocity $\delta\underline{u} = (u_1, w_1)$, of pressure p_1 and of concentration c_1 as:

$$(u_1, w_1, p_1, c_1) = (\delta u, \delta w, \delta p, \delta c)(z, t_0) \exp(\mathrm{i}ky) \exp(\sigma t), \tag{23}$$

where σ is the growth rate of the perturbations (since for our fronts $\omega(k)$ is purely imaginary, we use $\sigma = \mathrm{Im}\ \omega$ here) and k their wave number. Linearizing Eqs. (1)–(3) around the base state Eqs. (20)–(22) and eliminating w_1, p_1, we get the following linearized equations:

$$\left[\frac{\mathrm{d}^2}{\mathrm{d}z^2} - k^2\right] \delta u = k^2 \delta c, \tag{24}$$

$$\left[\frac{\mathrm{d}^2}{\mathrm{d}z^2} - v\frac{\mathrm{d}}{\mathrm{d}z} - \left.\frac{\mathrm{d}f}{\mathrm{d}c}\right|_{c_0} - \sigma - k^2\right] \delta c = \frac{\mathrm{d}c_0}{\mathrm{d}z} \delta u, \tag{25}$$

with δu and δc tending to zero for $z \to \pm\infty$. The problem is thus reduced to solving two coupled ordinary differential equations (24) and (25) that define an eigenvalue problem for σ, the solution of which gives the dispersion relation $\sigma = \sigma(k)$. We solve this eigenvalue problem by means of a second-order central finite-differencing scheme using the LAPACK solver DGEEVX [14]. There are three main methods to determine the stability of a time-dependent flow [28]. We have chosen the quasi-steady-state approximation over the solution of the initial value problem or the energy method. The quasi-steady-state approximation consists in freezing the base state at successive times and calculating the growth rate as if this corresponding base state was steady. This approximation is well justified here: if the front is pushed then, as explained before, the velocity converges exponentially fast to the asymptotic time-independent value; if, on the other hand, the front is pulled, then the convergence is so slow ($\sim 1/t$) that the quasistatic approximation is well justified too.

The first step is to create the one-dimensional RD front by solving Eq. (13) starting from a step function. This front $c_0(z, t)$ has a velocity $v(t)$ at a given time t at which the front snapshot is taken. In order to compute this front velocity at time t numerically, we follow as explained above a point of the front for which, say, $c = 0.5$, and calculate (numerically) the instantaneous velocity of this point. Even when the front velocity and shape are slowly relaxing for pulled fronts, to order $1/t^2$ all points of the front move with the same speed and the front shape relaxation is negligible; in other words, to this order

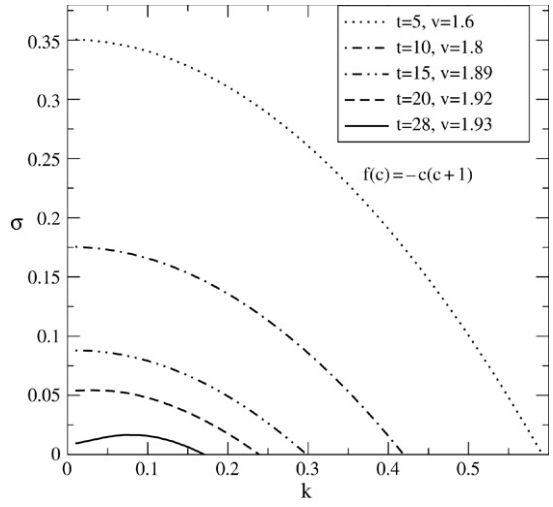

Fig. 7. Dispersion relation for the pulled front, computed at various successive times starting from an initial step function.

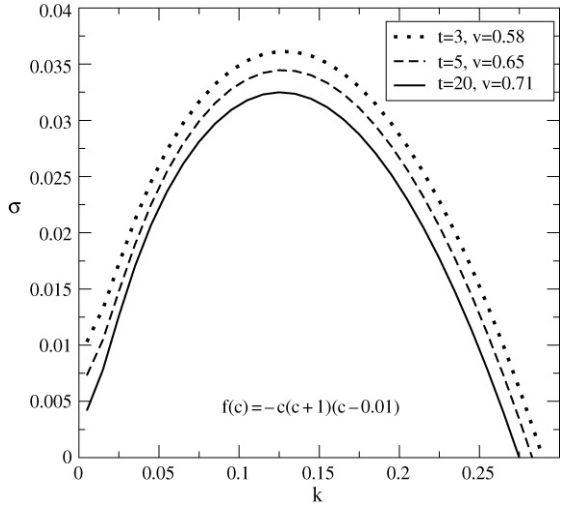

Fig. 8. Dispersion relation for the pushed front, computed at various successive times starting from an initial step function.

the front shape can be considered as the uniformly translating front solution associated with the instantaneous speed $v(t)$ [20, 21]. The profile $c_0(z, t)$ and the corresponding velocity $v(t)$ are then inserted into Eqs. (24) and (25) to compute the dispersion curve at time t.

The dispersion relations calculated this way are shown in Fig. 7 for the pulled case (6) and in Fig. 8 for the pushed case (7). The general behavior is indeed very much in line with what one expects from the scenario described above: the dispersion relation for the *pushed* case quickly converges to an asymptotic shape characteristic of the Rayleigh–Taylor instability, i.e. to a band of unstable modes ranging from $k = 0$ to a critical value k_c above which all modes are stable [9–15]. The most unstable mode k_m is such that $0 < k_m < k_c$. On the contrary, the dispersion relation of the *pulled* front keeps a strong time-dependence over all times. Moreover, the shape of the dispersion relation for pulled fronts changes dramatically: up to time of order 10 it has its maximum at $k = 0$ and the

growth rates are an order of magnitude larger than for pushed fronts, while only at later times does a gradual crossover to a weak Rayleigh–Taylor finite-wavelength instability relation become visible.

These results are simple to understand as follows. Note that according to (11) the velocity of a pulled front is always approaching the asymptotic value very slowly *from below*. Initially, therefore, the large maximum at $k = 0$ in the dispersion relation in the quasistatic approximation expresses the fact that the pulled front is still speeding up, and that the fastest growing mode of the intrinsic chemical front is the $k = 0$ mode. Only at very late times, when the asymptotic velocity v^* is almost reached, does the underlying Rayleigh–Taylor instability become apparent.

It is easy to make this idea more quantitative. In the leading edge of the chemical front, the asymptotic growth dynamics as a function of the time difference Δt is in leading order as

$$e^{(\sigma^* - Dk^2)\Delta t - \lambda^* z} \tag{26}$$

where D is given by (12). Now, in the quasistatic approximation, we probe the growth dynamics at time t in a comoving frame $z = v(t)\Delta t$. In this frame, the emerging mode (26) behaves as

$$e^{(\sigma^* - \lambda^* v(t) - Dk^2)\Delta t} \tag{27}$$

which corresponds to the time-dependent dispersion relation

$$\sigma(k, t) \approx \sigma^* - \lambda^* v(t) - Dk^2 = \lambda^*(v^* - v(t)) - Dk^2. \tag{28}$$

This expression (with in our case $v^* = 2$, $\lambda^* = 1$, $D = 1$) fits our numerical data reasonably well within 10%–15% error for not too large times, i.e. before the crossover to the Rayleigh–Taylor-like behavior. In fact, since this Rayleigh–Taylor instability is so much weaker (the maximal growth rate being of order 0.03), we can estimate the crossover time from the leading term in the asymptotic formula (11) as

$$\lambda^*(v^* - v(t_{\mathrm{cr}})) \approx \frac{3}{2t_{\mathrm{cr}}} \approx 0.03, \tag{29}$$

leading to $t_{\mathrm{cr}} \approx 50$. In practice the crossover time seems to be about a factor of 2 smaller. This is due to the fact that the leading-order term in the expression for $v^* - v(t)$ becomes accurate only for very late times, and the fact that the next-order correction term in the expansion is of opposite sign.

In conclusion, our results are a nice illustration of the fact that a pulled front, even if its thickness is small compared to the typical outer scale (a cell width, or the wavelength of an expected finite wavelength instability), cannot be mapped onto a moving boundary approximation. Because of the slow convergence of the intrinsic front velocity, there is a long initial transient during which the front is speeding up and has no finite wavelength instability. This conclusion applies quite generally, with the crossover time t_{cr} being longer the smaller the growth rate of the long-time finite wavelength instability is. These findings contrast strongly with the behavior in the pushed regime — there the intrinsic front speed converges exponentially fast to the asymptotic value, and the dispersion relation becomes essentially time-independent very quickly (Fig. 6).

One practical implication is that this long crossover is especially significant near the instability threshold; in finite-time simulations, this effect may therefore lead to an overestimation of the asymptotic stability of the front. This might be a reason for the difference in stability properties between an order two pulled kinetics and higher-order pushed kinetics noted by Coroian and Vasquez [18]. Unfortunately, insufficient information about the simulations in [18] is available to make quantitative estimates of the importance of such effects.

6. Conclusions

The pushed versus pulled character of traveling chemical fronts has long been recognized to lead to different reaction–diffusion dynamics and also to different sensitivity to the presence of fluctuations. We have here shown that, in addition, pulled and pushed RD fronts behave quite differently with regard to a Rayleigh–Taylor fingering instability setting in when an unfavorable density stratification acts across the front propagating vertically in the gravity field. Due to a very slow relaxation to the asymptotic front profile, pulled fronts are more sensitive initially to the diffusive mechanisms than to the convective modes when starting from an initial step function. As a consequence, their dispersion curves are strongly dependent on time at the onset of the instability and are characterized by a most unstable wavenumber centered around $k = 0$ before the dispersion curves of the Rayleigh–Taylor hydrodynamic modes set in at later times. In the nonlinear dynamics, the pulled system is very sensitive to the presence of fluctuations which can trigger onset of new traveling fronts ahead of the initial fronts in the presence of noise. On the contrary, pushed fronts relax rapidly to their asymptotic profile which translates into dispersion curves dominated by the hydrodynamic fingering modes even at early times. The nonlinear pushed fingers are robust with regard to fluctuations, which allows their fingering dynamics to be mapped into that of a sharp interface. This explains why the dispersion curves for the cubic kinetics of the iodate–arsenous acid reaction [9,11–13], the fourth-order kinetics of the chlorite–tetrathionate reaction [10,14,15] and more generally other typical pushed kinetics of order larger than two [18,19] all have similar properties. In the same spirit, their nonlinear dynamics [1–3,16] show similar features that could be mapped into a sharp interface description independently of the details of the pushed kinetics. This also suggests why the order two pulled kinetics studied by Vasquez et al. [18,19] in the framework of Rayleigh–Taylor fingering of fronts is characterized by a broader range of stability than the other pushed kinetics considered by these authors.

It is important to stress that the formal breakdown of the derivation of a moving boundary or thin front approximation for pulled fronts is quite subtle [8]. As a result, whether this result plays an important role or not depends very much on the problem at hand. Our own results are a good illustration of this:

while our pulled fronts were found to be effectively stable for a significant time, in the end, for long times, they exhibit the Rayleigh–Taylor instability. Other illustrations of this may be found in discharges [29] and combustion fronts [22,30], where fronts are pulled but where a moving boundary approximation in practice works quite well. On the other hand, pulled fronts may be quite sensitive to noise [20], and small lattice perturbations may drive a stable pulled reaction–diffusion front unstable [31]. Clearly, it really depends on the kind of question which is being asked, whether the fact that the dynamics of a front is pulled, plays up.

As fingering of pushed kinetics have already been quite well studied both experimentally and theoretically, it would be nice to welcome now an experimental analysis of pulled fronts to verify the predictions we give here. We stress that our results are not only valid for the specific reaction kinetics considered in the literature, but they do hold for pulled and pushed fronts in general. In particular, they immediately carry over to combustion, a field in which problems similar to those addressed in the chemical reaction literature have been studied recently (see [20,30,32] and references therein).

Acknowledgments

D.L. and A.D. wish to thank the Prodex programme (Belgium) of ESA for financial support and Serafim Kalliadasis for providing us a code to compute dispersion curves. A.D. acknowledges support of the Communauté française de Belgique (“Actions de Recherches Concertées” programme). We are also grateful to John Merkin for illuminating comments.

References

[1] A. De Wit, Phys. Fluids 16 (2004) 163.
[2] M. Böckmann, S.C. Müller, Phys. Rev. E 70 (2004) 046302.
[3] T. Bánsági Jr, D. Horváth, Á. Tóth, Chem. Phys. Lett. 384 (2004) 153.
[4] P.C. Fife, Dynamics of Internal Layers and Diffusive Interfaces, SIAM, Philadelphia, 1988.
[5] J.D. Buckmaster, G.S.S. Lundford, Theory of Laminar Flames, Cambridge UP, Cambridge, 1982.
[6] G. Caginalp, P. Fife, Phys. Rev. B 34 (1986) 4940.
[7] A. Karma, W.-J. Rappel, Phys. Rev. E 57 (1998) 4323.
[8] U. Ebert, W. van Saarloos, Phys. Rep. 337 (2000) 139.
[9] M. Böckmann, S.C. Müller, Phys. Rev. Lett. 85 (2000) 2506.
[10] D. Horváth, T. Bánsági Jr, A. Tóth, J. Chem. Phys. 117 (2002) 4399.
[11] A. De Wit, Phys. Rev. Lett. 87 (2001) 054502.
[12] J. Martin, N. Rakotomalala, D. Salin, M. Böckmann, Phys. Rev. E 65 (2002) 051605.
[13] R. Demuth, E. Meiburg, Phys. Fluids 15 (2003) 597.
[14] J. Yang, A. D’Onofrio, S. Kalliadasis, A. De Wit, J. Chem. Phys. 117 (2002) 9395.
[15] D.A. Vasquez, A. De Wit, J. Chem. Phys. 121 (2004) 935.
[16] D. Lima, A. D’Onofrio, A. De Wit, J. Chem. Phys. 124 (2006) 014509.
[17] S.K. Scott, K. Showalter, J. Phys. Chem. 96 (1992) 8702.
[18] D.I. Coroian, D.A. Vasquez, J. Chem. Phys. 119 (2003) 3354.
[19] D.A. Vasquez, E. Thoreson, Chaos 12 (2002) 49.
[20] W. van Saarloos, Phys. Rep. 386 (2003) 29.
[21] U. Ebert, W. van Saarloos, Physica D 146 (2000) 1.
[22] N. Vladimirova, R. Rosner, Phys. Rev. E 67 (2003) 066305.
[23] C.T. Tan, G.M. Homsy, Phys. Fluids 31 (1988) 1330.
[24] G.M. Homsy, Ann. Rev. Fluid Mech. 19 (1987) 271.
[25] D.J. Needham, J.H. Merkin, Nonlinearity 5 (1992) 413.
[26] J.A. Leach, D.J. Needham, Matched Asymptotic Expansions in Reaction–Diffusion Theory, Springer, Berlin, 2004.
[27] Ya.B. Zeldovich, G.I. Barenblatt, V.B. Librovich, G.M. Mkhviladze, The Mathematical Theory of Combustion and Explosions, Consultants Bureau, New York, 1965.
[28] C.T. Tan, G.M. Homsy, Phys. Fluids 29 (1986) 3549.
[29] M. Arayas, U. Ebert, Phys. Rev. 69 (2004) 036214.
[30] N. Vladimirova, R. Rosner, Phys. Rev. E 71 (2005) 067303.
[31] D.A. Kessler, H. Levine, Nature 394 (1999) 556.
[32] H. Berestycki, L. Kagan, S. Kamin, G. Sivashinsky, Int. Free Bound 6 (2004) 423.